MAIAC Thermal Technique for Smoke Injection Height from MODIS

Alexei Lyapustin, Yujie Wang, Sergey Korkin, Ralph Kahn, and David Winker

***Abstract*— We present a new algorithm to derive smoke plume height (H^a) using thermal contrast from the rising mixture of aerosol and emitted gases in the MODIS 11µm channel. Validation shows good agreement with wind-corrected MISR-MINX values, with about 60% of the MODIS Terra thermal retrievals within 500m of MISR H^a, and 450m lower on average. The bias is expected because the thermal technique represents an effective rather than a top plume height from MISR MINX. Comparison of MODIS Aqua retrievals with CALIOP CALIPSO shows similar statistics, with standard deviation of 458m for the mean plume height and 216m lower on average. H^a is part of the MAIAC MODIS Collection 6 suite of products (MCD19), accessible via the Land Product Distributed Active Archive Center (LP DAAC). Aerosol injection height is reported in the daily MAIAC atmospheric product MCD19A2 along with the cloud mask, column water vapor, aerosol optical depth, AOD uncertainty and aerosol type, at 1km resolution on global Sinusoidal grid. Despite some limitations, the vastly increased coverage from MODIS observations makes it a valuable dataset complementing the established MISR and CALIOP products.**

***Index Terms*—**Electromagnetics and Remote Sensing, Atmosphere < Methodologies and Applications to.

I. Introduction

WILDFIRE smoke plume height (H^a) is an important parameter for constraining aerosol chemical transport models in GCMs. It determines whether emitted smoke is a localized phenomenon limited to the atmospheric boundary layer, or is injected into a free troposphere and can travel long distances. Plume height information is required for modeling local and regional aerosol transport, air-quality, etc. Knowledge of injection height is particularly important for modeling plume-rise of energetic fires, which is associated with large uncertainties; model representations of small fires with low injection heights is much better constrained.

Plume height or "aerosol layer altitude", respectively, are currently available from two satellites: the Multi-angle Imaging Spectroradiometer (MISR) aboard the NASA Terra satellite [1], [2] and the Cloud-Aerosol LiDAR with Orthogonal Polarization (CALIOP) aboard the Cloud-Aerosol LiDAR and Infrared Pathfinder Satellite Observations (CALIPSO) [3], [4]. Although these satellites provide planet-wide observations, they are limited in temporal frequency, with 16-day sub-spacecraft coverage for CALIOP and 9-day global coverage for MISR; as a result, many fires are missed. Although MISR plume heights are reported at 1.1 km horizontal resolution and CALIOP values are provided at up to 70 m, in a recent review of smoke injection height in large-scale atmospheric chemical transport models, [5] state that *"… determination of the injection heights at spatiotemporal scales … matching … active fire observations*" from the Moderate Resolution Imaging Spectroradiometer (MODIS) "*is more likely to rely on injection height parameterizations*" for many applications, due to the coverage limitations of MISR and CALIOP. Here, we present a new MODIS-based thermal technique for smoke injection height implemented in the Multi-Angle Implementation of Atmospheric Correction (MAIAC) algorithm [6]. The broad-swath MODIS instruments each cover the entire planet every 1-2 days. In this paper, we use the terms "injection height" and "plume height" interchangeably, though the latter is an approximation of the former near the source.

II. MAIAC Plume Height Algorithm

The recently described MAIAC algorithm [6] offers a unique infrastructure for smoke detection and characterization. It includes: 1) high quality cloud and snow detection; the cloud mask (CM) algorithm includes detection of thermal hotspots based on modified [7]; 2) detection of absorbing smoke and dust aerosols. The smoke test is optimally integrated with cloud detection in a way that minimizes cloud leak and preserves most of strong smoke plumes, which are usually filtered by cloud mask [6], [8], [9]; 3) aerosol optical depth (AOD) retrieval at high 1km resolution.

Rising aerosol plumes from wildfires often display a "colder" brightness temperature (T_b), representing its effective height above ground, and creating T_b contrast with the neighbor smoke-free ground pixels (ΔT_b). MAIAC smoke detection allows us to implement a simple aerosol plume height algorithm for pixels with detected smoke based on ΔT_b, under an assumed atmospheric temperature profile or an average lapse rate. Figure

Submitted April 23, 2019. The research of A. Lyapustin, Y. Wang and S. Korkin was funded by the NASA Science of Terra, Aqua, SNPP (17-TASNPP17-0116; solicitation NNH17ZDA001N-TASNPP). A. Lyapustin was additionally supported by the NASA GeoCAPE program.

A. Lyapustin and R. Kahn are with Laboratory for Atmospheres, NASA Goddard Space Flight Center, Greenbelt, Maryland, USA (e-mail: alexei.i.lyapustin@nasa.gov).

Y. Wang is with University of Maryland Baltimore County, Baltimore, Maryland, USA.

S. Korkin is with Universities Space Research Association, Columbia, Maryland, USA.

D. Winker is with 4NASA Langley Research Center, Hampton, Virginia, USA.

1 gives an illustration for the Rocky Mountain wildfires during summer 2008. The columns show the MODIS top-of-atmosphere (TOA) RGB image, MAIAC cloud mask (CM), aerosol optical depth at 470 nm (AOD0.47), 11µm brightness temperature (T_b) and derived plume height for an assumed lapse rate of 6.5° km^{-1}. Green color in the cloud mask panel shows detected fire hotspots. Each row corresponds to a different day of 2008, specifically 190, 191, 202 and 224. An arrow identifies the thermal contrast in the MODIS 11µm channel (band 31) created by the rising smoke plume on day 202. Several strong plumes are easily visible on day 224 in TOA RGB, AOD and Tb images.

The fine-mode aerosol particles generated by fires are not visible in the 11µm channel. The thermal contrast is created by

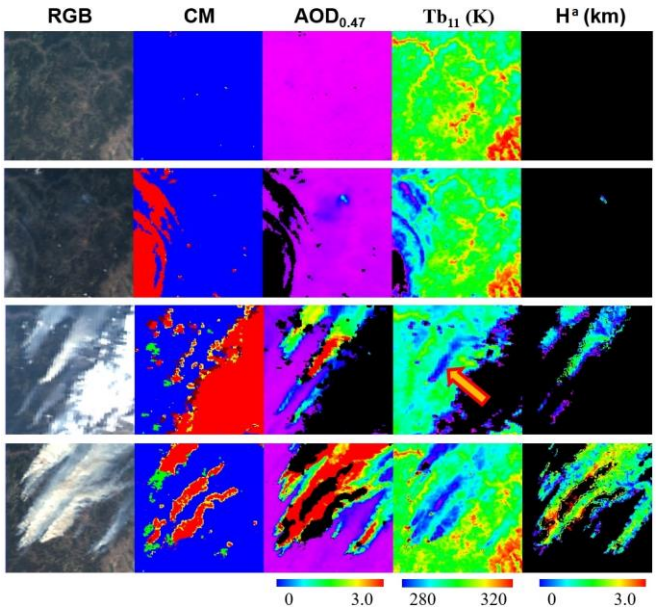


Fig. 1. Illustration of smoke plume height retrieval from MODIS for the Rocky Mountains wildfires of summer 2008. The columns show the MODIS TOA RGB image, MAIAC cloud mask (CM), aerosol optical depth (AOD), 11µm brightness temperature (Tb) and plume height above ground. The cloud mask legend is as follows: clear, cloud, shadow, detected fire. Each row corresponds to a different day of 2008, specifically 190, 191, 202 and 224. An arrow identifies the thermal contrast created by the rising smoke plume on Day 202.

several other physical mechanisms: the main one is absorption by gases entrained in the rising smoke plume and re-emission from the effective plume altitude. Although 11µm is considered an atmospheric window channel, there is absorption by carbon dioxide (CO_2), nitrous oxide (NO_2), ammonia (NH_3), methane (CH_4), water vapor and other gases released during combustion. Normally, absorption by these gases under background conditions is ~7-10%. Within wildfire plumes, the concentrations of these gases can be much higher than in the background atmospheric column, creating a significant absorption. Next, wildfires often release a considerable amount of water vapor that can condense into 5-10 µm liquid droplets at the top of aerosol plume. The resulting pyrocumulus clouds provide another source of thermal contrast. Other mechanisms that do not affect the current results include surface irradiance reduction by the smoke and cooling of the surface below compared to the smoke-free areas, e.g. [10].

MAIAC smoke detection [8], [11] is the key feature of the algorithm that allows MAIAC to by-pass cloud detection, retain most of the strongest plumes, and provide AOD at 1km resolution. Smoke height is evaluated for a pixel (i,j) with detected smoke if 1) the AOD at 0.47µm is sufficiently high (≥0.8), 2) an estimate of the ground brightness temperature T_{bG} for the smoke-free land surface is available, and 3) $\Delta T_b = T_{bG} - T_{b,ij} > 0$. When all three conditions are met, MAIAC computes plume height assuming a fixed lapse rate of 6.5° km^{-1}, $H^a = \Delta T_b/6.5$ (km).

The ground brightness temperature in MAIAC is computed as an average value for each 25×25km^2 block using cloud- and smoke-free pixels. If T_{bG} for the block containing pixel (i,j) is not available, we compute T_{bG} as a weighted average from a larger meso-scale (150km) area, where the weights are defined as an inverse squared distance. To account for the surface height variation in non-flat terrain, we compute T_{bG} for five surface-height bins, in increments of 0.5 km: 0-0.5km, … 2-2.5km, and use the appropriate T_{bG} bin corresponding to pixel (i,j) surface height.

The described thermal technique has several limitations. First, the emitted gas concentrations decrease over time, and with distance from the source of burning, due to dilution and chemical reactions in the gas phase, including oxidation, formation of secondary organic aerosol, heterogeneous reactions and coatings created on the primary organic, black- and brown carbon aerosol particles. The decrease of absorbing gas concentration leads to an increased "warmer" surface contribution to the TOA 11µm radiance signal, effectively pushing the "weighting function" toward the surface. The resulting reduction in thermal contrast could be interpreted incorrectly by this technique as a decrease in the plume height. This phenomenon limits application of the thermal technique to a certain "dissipation" distance from the source. Second, our approach does not work when the smoke area is very large and T_{bG} cannot be estimated reliably. Finally, the thermal technique is not designed for small fires, having low emission of absorbing gases and lack of thermal contrast. The empirical threshold AOD>0.8 helps to filter these cases.

The algorithm presented also employs two main simplifications. First is the use of the average lapse rate of 6.5° km^{-1} instead of an atmospheric temperature profile from climate or weather forecast models. This simplification was adopted initially because a) in the absence of a dense radiosonde network, profiles from different models may not agree, indicating general uncertainty, and b) MODIS operational processing uses forecast, whereas re-analysis available several hours later would provide more accurate atmospheric profiles. Thus, our approach allows an experienced user to re-scale the H^a value back to the ΔT_b contrast and derive a more accurate aerosol height estimate with a user-selected profile. If used as is, MAIAC H^a accuracy is somewhat reduced and can contain regional and seasonal biases. The second simplification is the use of the brightness temperature for the background characterization, which assumes the surface emissivity (ε=1). The emissivity in MODIS band 31 (11µm) ranges from 0.92-1 [12], and is rather stable over vegetated surfaces (ε~0.97-0.98)

where fires occur. Lower values are found over deserts and semi-arid/arid areas. At a surface temperature T=300K with ε~0.975, the assumption ε =1 will bias T_{bG} by approximately 1.7°K and reduce retrieved height by about 260m. Finally, absorption of water vapor emitted by fire can add to uncertainty in our approach.

III. Comparison with MISR and CALIOP Data

A specialized MISR Interactive eXplorer (MINX) program uses optical parallax along with operator input of source location, wind direction, and plume area to derive H^a, e.g. [2]. Wind-corrected plume heights from MISR MINX have an accuracy of 250-500m. We compared MAIAC H^a from MODIS Terra with coincident MISR-MINX values for 1089 plumes over North America from 2000-2008 [13] (https://misr.jpl.nasa.gov/getData/accessData/MisrMinxPlumes2/). Statistical analysis of these cases is shown in Figure 2 in histograms of (a) the H^{MISR}-H^{MODIS} height difference distribution ("fixed lapse rate" shown by the red solid line) and (b) the standard deviations of retrieved heights for each algorithm. MAIAC values are lower by about 200m at the peak of histogram, and by 448m on average. In addition to MAIAC's systematic bias from the neglect of surface emissivity, the effective plume heights from MAIAC are expected to be lower than MISR values, which generally relate to plume-top (though a distribution of heights giving some indication of plume vertical extent is usually obtained; e.g. [1]. 59.3% of MAIAC plume heights are found within ±500m of the MISR-MINX values. MAIAC-retrieved plume heights show smaller standard deviation, σ_H=179m, vs. 300m for MISR. This comparison indicates good agreement, given the uncertainties of both datasets, including a singularity in the MISR approach when the plume and satellite orbit directions closely align [2], simplifications in the MAIAC technique, and differences in the vertical sampling of these methods. It is also worth mentioning that generating MISR MINX dataset for 1089 fires required operator fire detection and other input whereas MAIAC retrievals were available automatically with exception of small fires.

In addition, MAIAC H^a values from MODIS Aqua were compared with data from CALIOP on the CALIPSO satellite, that orbit together in the A-train constellation. We used the version 4.10 "Lidar Level 2 Cloud and Aerosol Layer Products" reported at 5km resolution. Similar to [14], we find that MAIAC heights are significantly lower than the CALIOP layer top altitude, even when a single layer was reported. Due to CALIOP sensitivity to high-altitude aerosol layers, extinction-weighted values, as in [14], did not yield good comparisons either. Better agreement is obtained when the CALIOP "height" is derived as the average between the reported layer top and base altitudes, corrected for the surface elevation. For multi-layer cases, the average height of the optically thickest layer with the highest "Feature_Optical_Depth_532" is used. The CALIOP data were excluded when the feature optical depth was a factor of ≥3 larger or smaller than corresponding MAIAC AOD value. For each 5km CALIOP box, the MAIAC H^a value is represented by the maximal retrieved height within the nested 1km MAIAC grid. The co-location error due to the 1-2 min overpass time difference between MODIS Aqua and CALIPSO amounts to ±5km. To mitigate uncertainties from co-location and other sources, we also compare the values averaged over the transect length of individual plumes. To mitigate MAIAC uncertainties from ground brightness temperature characterization, this analysis was limited to well-defined smoke plumes close to the emission source. These were identified based on detected thermal hotspots and a sharp boundary in MAIAC AOD, dropping to the background level within a ±75km region. This automated analysis over the North America from 2006 to 2017 identified 404 5km boxes and 76 individual plumes with matched MODIS Aqua – CALIOP retrievals.

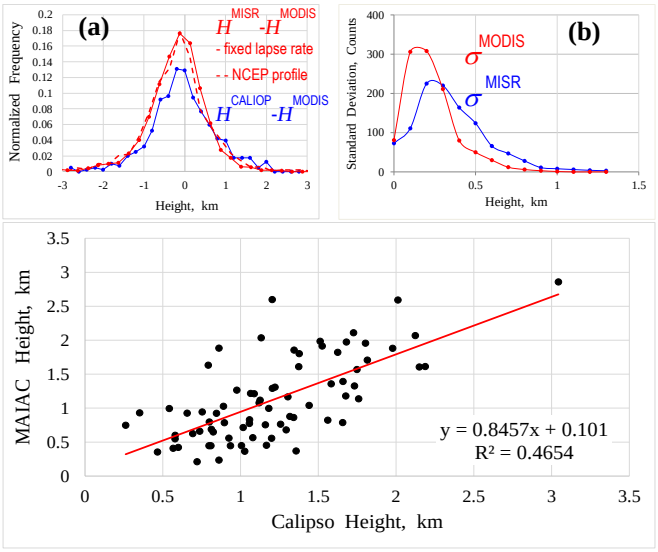


Fig. 2. (a) Histograms of MODIS Terra-MISR, and MODIS Aqua – CALIOP – 5km plume height differences; (b) standard deviations of retrieved plume heights for MODIS Terra and MISR, and (c) scatterplot of MODIS Aqua – CALIOP plume heights averaged over transects of individual fires.

Results from this comparison are shown in Figure 2 a) and c). As with the MISR MINX results: MAIAC thermal H^a agree with the CALIPSO values to within measurement uncertainties, on average 216m lower, with a standard deviation of 458m for the plume-averaged transects. When considering the larger statistics for 5km boxes, the standard deviation is higher (851m). Previous studies found CALIPSO plume-top heights generally higher than MISR, due primarily to differences in instrument sensitivities to very thin aerosol [15], [16]. The current analysis applies a definition of CALIPSO plume height that averages layer top and bottom heights. This significantly lowers the effective CALIPSO values and accounts for MAIAC H^a appearing on average 458m below MISR, but only 216m below CALIPSO.

To evaluate effect of the fixed lapse rate assumption, we re-calculated MAIAC H^a using the National Center for Environmental Predictions (NCEP) temperature profiles [17] available as part of the MODIS ancillary dataset. The result of comparison with MISR MINX is presented in Figure 2a by the dashed line. It shows that, indeed, the use of the realistic

temperature profiles narrows the histogram of the MODIS – MISR height difference by about 10% in approximately half of all cases, thus improving the agreement. On the other hand, we did not observe an improved agreement with CALIPSO, which may be explained by several factors, including our definition of CALIPSO height, a rather coarse 1°×1° resolution of the NCEP profiles, which creates uncertainty over non-flat terrains, and the fundamental differences in the sensitivities of the two instruments.

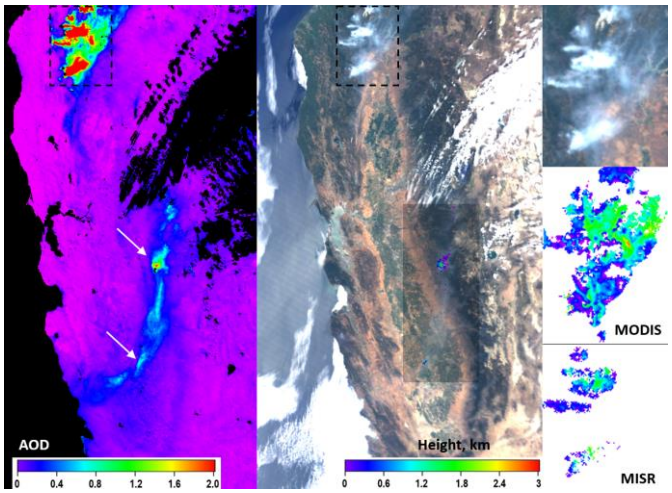


Fig. 3. Illustration of retrievals for California fires on July 29, 2008. Shown from left to right are MAIAC AOD, MODIS Terra RGB image, and MODIS Terra and MISR MINX injection height retrievals for northern California. Arrows in the AOD image indicate the locations of additional MAIAC height retrievals for the California Central Valley that appear as darker overlays in the MODIS RGB image but were not digitized for the MISR MINX database.

IV. Spatial Coverage

To evaluate retrieval coverage, we compared plume height retrieval statistics from MODIS Terra and MISR over North America for 2018. When considering the area covered by valid MISR MINX retrievals, the statistics are nearly identical: 25087 vs 25002 pixels with valid plume heights from MISR and MODIS Terra, respectively. MAIAC does not provide retrievals for some small fires captured by MISR, but as MAIAC reports the large fires over a greater area, the total MAIAC retrieval count is comparable to that of MISR. An example of such retrievals for the northern California on July 29, 2008 is shown in Figure 3.

For the area covered by the MISR field of view (380km swath width), MAIAC reports about a factor of 20 more plume height retrievals than MISR. The difference mostly represents transported smoke far from the emission sources that the MISR-MINX operator most likely did not choose to digitize, but were nevertheless captured by the automatic MODIS algorithm. A separate validation of these retrievals with CALIOP data shows a lack of correlation in general, although about 20% of the data are in a good agreement. Because at present we cannot identify which MAIAC retrievals have a good quality in places where neither MISR nor CALIOP validation data are available, the use of this height product for transported smoke is not recommended. It should be mentioned that the MISR MINX technique can be applied to the transported smoke, in addition to the current focus on the rising plumes from active fires. This analysis, therefore, shows that the current coverage of well understood thermal MODIS Terra retrievals and MISR for the active fire plumes is very similar per unit area.

For the full MODIS swath (2330km), the coverage difference with MISR grows in proportion to the area observed. It is interesting to note that the Aqua record features about 60% more detected hotspots by MAIAC and 14% more smoke height retrievals than Terra. This is consistent with the expected increase in fire energy from late morning to early afternoon. In summary, with the exception of small fires, MAIAC MODIS provides reliable retrievals with similar coverage per unit area to that of MISR. However, it offers more retrievals due to the larger MODIS swath width, and coverage is increased further as there are two MODIS sensors on orbit.

V. Conclusion

We present a new algorithm to derive smoke plume height using thermal contrast created by the rising mixture of aerosol and emitted gases in the MODIS 11μm channel. The thermal technique is simple and robust once clouds and smoke aerosol are reliably detected by MAIAC MODIS processing. Validation shows good agreement with wind-corrected MISR-MINX values, with about 60% of MAIAC retrievals within 500m of MISR H^a, and skewed 450m lower on average. The bias is expected in part because the thermal technique represents effective rather than peak-weighted plume height, and in part because MAIAC currently neglects non-unit surface emissivity. CALIOP validation of MODIS Aqua retrievals shows similar statistics, namely underestimation on average by 216m with the standard deviation of 458m for plume-averaged transects. The validation also shows that the retrievals are of comparable quality to MISR MINX for rising plumes in proximity of active fires, but they are not as reliable for transported smoke.

MAIAC MODIS Collection 6 processing has been completed and its product suite (MCD19) is accessible via the Land Product Distributed Active Archive Center (LP DAAC). Aerosol injection height is reported in the daily MAIAC atmospheric product MCD19A2 along with the cloud mask, column water vapor, aerosol optical depth, AOD uncertainty and aerosol type, at 1km resolution on a global Sinusoidal grid. The reported H^a can be either used directly, or re-computed using user-specified temperature profiles, for example from MERRA2 re-analysis (https://gmao.gsfc.nasa.gov/reanalysis/MERRA-2/). MERRA-2 profiles and MODIS land surface emissivity, which recently became available from MODIS Aqua MYD21 product [12] at 1km resolution, will be implemented in the next version of MAIAC algorithm. To exclude transported smoke and ensure good quality of retrievals, we currently recommend to use H^a within ~75-150km from the detected thermal hotspots as reported in the MAIAC quality assurance (QA) flag in MCD19A2 product.

Although there are certain limitations to the technique presented, as discussed in section 2, the vastly increased coverage proportional to the observation coverage and at least

partial representation of the diurnal cycle from the ~10:30 AM (Terra) and ~1:30 PM (Aqua) MODIS observations makes it a valuable dataset complementing the established MISR and CALIOP products. The technique is generic and will be extended to the Suomi-NPP and J1 VIIRS measurements. A prototype algorithm has also been developed for the geostationary AHI-8 HIMAWARI data.

ACKNOWLEDGMENT

The following datasets were used in this work

- "MAIAC MODIS atmospheric products (MCD19A2)", doi:10.5067/MODIS/MCD19A2.006

-"MISR MINX Plume Height", https://misr.jpl.nasa.gov/getData/accessData/MisrMinxPlumes2/

- "CALIOP v4.10 "Lidar Level 2 Cloud and Aerosol Layer Products", doi:10.5067/CALIOP/CALIPSO/LID_L2_05kmALay-Standard-V4-20.

REFERENCES

[1] R. A. Kahn, W. H. Li, C. Moroney, D. J. Diner, J. V. Martonchik, and E. Fishbein, "Aerosol source plume physical characteristics from space-based multiangle imaging", *Journal of Geophysical Research*, vol. 112, D11205, 2007, doi:10.1029/2006JD007647.

[2] D. L. Nelson, M. J. Garay, R. A. Kahn, and B. A. Dunst, "Stereoscopic Height and Wind Retrievals for Aerosol Plumes with the MISR INteractive eXplorer (MINX)", *Remote Sensing*, vol. 5, 4593-4628, 2013. doi:10.3390/rs5094593.

[3] D. Winker D., M. Vaughan, A. Omar, Y. Hu, K. Powell, Z. Liu, W. Hunt, and S. Young, "Overview of the CALIPSO Mission and CALIOP Data Processing Algorithms", *Journal of Atmospheric and Oceanic Technology*, vol. 26, pp. 2310–2323, 2009, doi: 10.1175/2009JTECHA1281.1.

[4] M. Labonne, F. M. Breon, and F. Chevallier, "Injection height of biomass burning aerosols as seen from a spaceborne LiDAR", *Geophysical Research Letters*, vol. 34, L11806, 2007, doi:10.1029/2007GL029311.

[5] R. Paugam, M. Wooster, S. Freitas, M. Val Martin, "A review of approaches to estimate wildfire plume injection height within large-scale atmospheric chemical transport models", Atmospheric Chemistry and Physics, vol. 16, pp. 907–925, 2016, doi:10.5194/acp-16-907-2016.

[6] A. Lyapustin, Y. Wang, S. Korkin, and D. Huang, "MODIS Collection 6 MAIAC Algorithm", *Atmospheric Measurement Techniques*, vol.11, pp.5741-5765, 2018, https://doi.org/10.5194/amt-2018-141.

[7] L. Giglio, W. Schroeder, and C. O. Justice, "The collection 6 MODIS active fire detection algorithm and fire products", *Remote Sens. Environ.*, vol. 178, pp. 31–41, 2016, https://doi.org/ 10.1016/j.rse.2016.02.054.

[8] A. Lyapustin, S. Korkin, Y. Wang, B. Quayle, and I. Laszlo, Discrimination of biomass burning smoke and clouds in MAIAC algorithm, *Atmospheric Chemistry and Physics*, vol. 12, pp. 9679–9686, 2012, doi:10.5194/acp-12-9679-2012.

[9] I. Veselovskii, D. Whiteman, M. Korenskiy, A. Suvorina, A. Kolgotin, A. Lyapustin, Y. Wang, M. Chin, H. Bian, T. L. Kucsera, D. Pérez-Ramírez, and B. Holben, "Characterization of forest fire smoke event near Washington, DC in summer 2013 with multi-wavelength lidar", *Atmos. Chem. Phys.*, vol. 15, 1647-1660, 2015, doi:10.5194/acp-15-1647-2015.

[10] J. Zhang, J. S. Reid, M. Christensen, and A. Benedetti, "An evaluation of the impact of aerosol particles on weather forecasts from a biomass burning aerosol event over the Midwestern United States: observational-based analysis of surface temperature", *Atmos. Chem. Phys.*, vol. 16, 6475-6494, 2016, doi: 10.5194/acp-16-6475-2016.

[11] A. Lyapustin, Y. Wang, I. Laszlo, R. Kahn, S. Korkin, L. Remer, R. Levy, and J. S. Reid, J. S, "Multi-Angle Implementation of Atmospheric Correction (MAIAC): Part 2. Aerosol Algorithm", *Journal of Geophysical Research*, vol. 116, D03211, 2011, doi:10.1029/2010JD014986.

[12] G. C. Hulley, and S. J. Hook, "Generating Consistent Land Surface Temperature and Emissivity Products Between ASTER and MODIS Data for Earth Science Research", *IEEE Transactions on Geoscience and Remote Sensing*, vol. 49, 1304-1315, 2011, 10.1109/TGRS.2010.2063034.

[13] M. Val Martin, J. A. Logan, R. A. Kahn, F. Y. Leung, D. L. Nelson,and D. J. Diner, "Smoke injection heights from fires in North America: analysis of 5 years of satellite observations", *Atmospheric Chemistry and Physics*, vol. 10, 1491–1510, 2010, doi:10.5194/ACP-10-1491-2010.

[14] M. G. Tosca, J. T. Randerson, C. S. Zender, D. L. Nelson, D. J. Diner, and J. A. Logan, "Dynamics of fire plumes and smoke clouds associated with peat and deforestation fires in Indonesia", *J. Geophys. Res.*, vol. 116, D08207, 2011, doi:10.1029/2010JD015148.

[15] R. A. Kahn, Y. Chen, D. L. Nelson, F. Y. Leung, Q. Li, D. J. Diner, and J. A. Logan, "Wildfire smoke injection heights–two perspectives from space", *Geophysical Research Letters*, vol. 35, L04809, 2008, doi:10.1029/2007GL032165.

[16] V. Flower, and R. A. Kahn, "Assessing the altitude and dispersion of volcanic plumes using MISR multi-angle imaging: Sixteen years of volcanic activity in the Kamchatka Peninsula, Russia", *J. Volcanology and Geothermal Research*, vol. 337, pp. 1–15, 2017, https://doi.org/10.1016/j.jvolgeores.2017.03.010.

[17] E. Kalnay, M. Kanamitsu, and W.E. Baker, "Global Numerical Weather Prediction at the National-Meteorological-Center." *Bulletin of the American Meteorological Society, 71*, 1410-1428, 1990.